DOI 10.47176/sjfst.4.2.1

Original Article

SRPH

SJFST, 2022; 4(2): 1-14

A Creep and Shrinkage Prediction Model for Serviceability Analysis of Composite Concrete Slabs with Steel Decking

Alireza Gholamhoseini*

Lead Structural Engineer, Orion Structural Consulting, Auckland, New Zealand.

***Corresponding Author:**
gholamhoseinia@gmail.com

Received: 15 February, 2022
Accepted: 05 April, 2022
Published: 10 April, 2022

ABSTRACT

The Relatively little research has been reported on the time-dependent in-service behavior of composite concrete slabs with profiled steel decking as permanent formwork and little guidance is available for calculating long-term deflections. The drying shrinkage profile through the thickness of a composite slab is greatly affected by the impermeable steel deck at the slab soffit, and this has only recently been quantified. This paper presents the results of long-term laboratory tests on composite slabs subjected to both drying shrinkage and sustained loads. Based on laboratory measurements, a design model for the shrinkage strain profile through the thickness of a slab is proposed. The design model is based on some modifications to an existing creep and shrinkage prediction model B3. In addition, an analytical model is developed to calculate the time-dependent deflection of composite slabs taking into account the time-dependent effects of creep and shrinkage. The calculated deflections are shown to be in good agreement with the experimental measurements.

Keywords: Composite slabs, Creep, Deflection, Profiled steel decking, Serviceability, Shrinkage

Introduction

Composite one-way concrete floor slabs with profiled steel decking as permanent formwork are commonly used in the construction of floors in buildings (Fig. 1a). The steel decking supports the wet concrete of a cast in-situ reinforced or post-tensioned concrete slab and, after the concrete sets, acts as external reinforcement. Embossments on the profiled sheeting provide the necessary shear connection to ensure composite action between the concrete and the steel deck (Fig. 1b).

Despite their common usage, relatively little research has been reported on the in-service behavior of composite slabs. In particular, the drying shrinkage profile through the slab thickness (which is greatly affected by the impermeable steel decking) and the restraint to shrinkage provided by the steel decking have only recently been quantified [1-5]. Carrier et al. [6] measured the moisture contents of two bridge decks, one was a composite slab with profiled steel decking and the other was a conventional reinforced concrete slab permitted to dry from the top and bottom surfaces after the timber forms were removed. The moisture loss was significant only in the top 50 mm of the slab with profiled steel decking and in the top and bottom 50 mm of the conventionally reinforced slab. In their research, Gilbert et al. [1] measured the nonlinear variation of shrinkage strain through the thickness of several slab specimens, with and without steel decking at the soffit, and sealed on all exposed concrete surfaces except for the top surface. Ranzi et al. [2] carried out long-term tests on a post-tensioned solid concrete slab and two composite slabs with two different steel decking types and also measured the occurrence of non-uniform shrinkage strain through the thickness of the two composite slabs. Bradford [7] presented a generic model for composite slabs subjected to concrete creep and two types of indirect (or non-mechanical) straining effects; shrinkage and thermal strains; including the effects of partial interaction between the concrete slab and steel decking.

[Downloaded from sjfst.srpub.org on 2026-09-16]

[DOI: 10.47176/sjfst.4.2.1]

Publisher: Scientific Research Publishing House (SRPH), Shirvan, Iran
http://srpub.org
Email: sjfst@srpub.org

(a) Soffit of a one-way composite slab and beam floor system

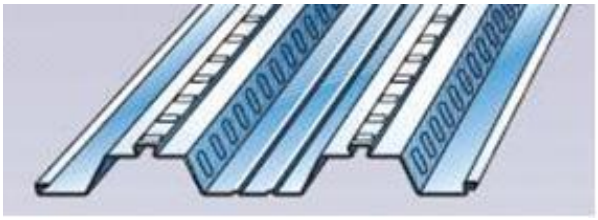

(b) Trapezoidal steel decking profile KF70

Figure 1. Profiled steel decks (Fielders Australia)

As a consequence of the dearth of published research, little design guidance is available to structural engineers for predicting the in-service deformation of composite slabs. The techniques used to predict deflection and the on-set of cracking in conventionally reinforced concrete slabs [8-9] are often applied inappropriately. Although techniques are available for the time-dependent analysis of composite slabs [9], due to lack of guidance in codes of practice, structural designers often specify the decking as sacrificial formwork, in lieu of timber formwork, and ignore the structural benefits afforded by the composite action. Of course this provides a conservative estimate of ultimate strength of the slab and is quite unsustainable, but may well result in a significant under-estimation of deflection because of the shrinkage strain gradient and the restraint provided by the deck and this should not be ignored.

In this paper, the results of an experimental study of the long-term deflection of composite concrete slabs due to sustained service loads and shrinkage are presented. Deflections caused by creep of the concrete and the effects of drying shrinkage are reported and discussed. Based on the experimental results, a shrinkage strain profile is proposed based on some modifications to Bazant-Baweja B3 model [10] for prediction of creep and shrinkage for design purposes and an analytical technique is proposed for determining the time-varying deflections of composite floor slabs with profiled steel decking. Good agreement is obtained between the calculated and measured deflections.

Experimental Program

The experimental program involved the testing of ten large scale simple-span composite one-way slabs under different sustained, uniformly distributed service load histories for periods of up to 244 days. Two different decking profiles KF40 and KF70 [12] were considered as shown in Fig. 2.

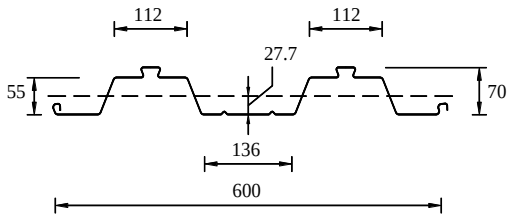

A_{sd} = 1100 mm²/m; y_{sd} = 27.7 mm; I_{sd} = 584000 mm⁴/m

(a) KF70

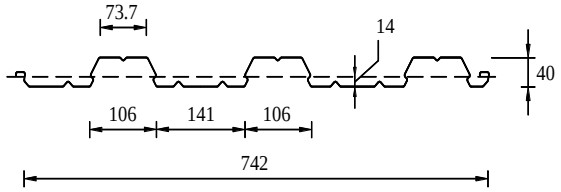

A_{sd} = 1040 mm²/m; y_{sd} = 14.0 mm; I_{sd} = 269000 mm⁴/m

(b) KF40

Figure 2. Dimensions (in mm) of each steel decking profile (t_{sd} =0.75 mm)

[Downloaded from sjfst.srpub.org on 2026-09-16]

[DOI: 10.47176/sjfst.4.2.1]

The creep coefficient and drying shrinkage strain for the concrete were measured on companion specimens cast with the slabs and cured similarly. Additionally, the compressive strength and the elastic modulus of concrete at the age of first loading and at the end of the sustained load period were measured on standard 100 mm diameter cylinders; while the concrete flexural tensile strength (modulus of rupture) was measured on 100 mm × 100 mm × 500 mm concrete prisms. The elastic modulus E_{sd} and the yield stress f_y of the steel decking were also measured on coupons cut from the decking.

Crack locations and crack widths on the side surfaces of the slabs were recorded throughout the long-term test, together with the time-dependent change in concrete and steel strains, mid-span deflection and the slip between the steel decking and the concrete at each end of the specimen.

The objectives of the experimental program were to obtain benchmark, laboratory-controlled data on the long-term structural response of composite slabs under different sustained service loads, in particular the time-varying deflection, and to analyze the effect of creep and shrinkage on the long-term behavior of composite slabs. The laboratory data was then used to validate analytical models for the prediction of time-dependent behavior [1, 9] and to assist in the development of design-oriented procedures to assess the serviceability of composite slabs.

Test Specimens and Instrumentation

Each slab was 3300 mm long, with a cross-section 150 mm deep and 1200 mm wide, and contained no reinforcement (other than the external steel decking). Each slab was tested as a single simply-supported span. The center to center distance between the two end supports (one hinge and one roller) was 3100 mm. Five identical slabs with KF70 decking were poured at the same time from the same batch of concrete. An additional five identical slabs with KF40 decking were poured at a different time from a different batch of concrete (but to the same specification and from the same supplier). The thickness of the steel sheeting in both types of decking was t_{sd} = 0.75 mm. The cross-section of each of the five slabs with KF70 decking is shown in Fig. 3a. The choice of specimen variables was made in order to examine the effects of shrinkage and sustained load levels on long-term deflections for slabs with two different deck profiles, while keeping slab thickness and concrete properties the same for each specimen. Further testing will be necessary to consider the effects of varying the concrete properties and slab thickness on long-term deflection.

Each slab was covered with wet hessian and plastic sheets within four hours of casting and kept moist for six days to delay the commencement of drying. At age 7 days, the side forms were removed and the slabs were lifted onto the supports. Subsequently, the slabs were subjected to different levels of sustained loading provided by means of different sized concrete blocks. A photograph of the five KF70 slabs showing the different loading arrangements and the slab designations are also shown in Fig. 4. The first digit in the designation of each slab is the specimen number (1 to 10) and the following two letters indicate the nature of the test, with LT for long-term. The next two numbers indicate the type of decking (with 70 and 40 for KF70 and KF40, respectively). The final digit indicates the approximate value of the maximum superimposed sustained loading in kPa.

The mid-span deflection of each slab was measured throughout the sustained load period with dial gauges at the soffit of the specimen. Dial gauges were also used to measure the slip between concrete slab and steel decking at the ends of the slab at both roller and hinge supports in slabs 2LT-70-3, 3LT-70-3, 4LT-70-6 and 5LT-70-8 with KF70 decking and in slabs 7LT-40-3 and 9LT-40-6 with KF40 decking. At the mid-span of each slab, the concrete strains were measured on the top and bottom surfaces using 60 mm long strain gauges. The strain gauges were glued onto the concrete surface and steel sheeting after removing the wet hessian at age 7 days. Internal embedded wire strain gauges were used to measure the concrete strains at different depths through the thickness of slabs 2LT-70-3, 5LT-70-8, 7LT-40-3 and 9LT-40-6, with locations shown on the cross-section in Fig. 3b. The self-weight and cross-sectional properties of the composite slabs are given in Table 1.

The location, height and width of the cracks were measured on the side faces of each specimen and recorded throughout the test. Of particular interest was the time-dependent development of cracking and the increase in crack widths with time. Crack widths were measured using a microscope with a magnification factor of 40. The average relative humidity (*RH*) in the laboratory throughout the period of testing was 67% and 72% for the KF70 and KF40 test specimens, respectively.

Table 1
Properties of composite slabs

Slab Decking Profile	Slab Self-Weight (kPa)	Gross Section I_g (mm^4)	Cracked Section I_{cr} (mm^4)
KF70	3.0	278×10^6	102×10^6
KF40	3.2	310×10^6	111×10^6

[Downloaded from sjfst.srpub.org on 2026-09-16]

[DOI: 10.47176/sjfst.4.2.1]

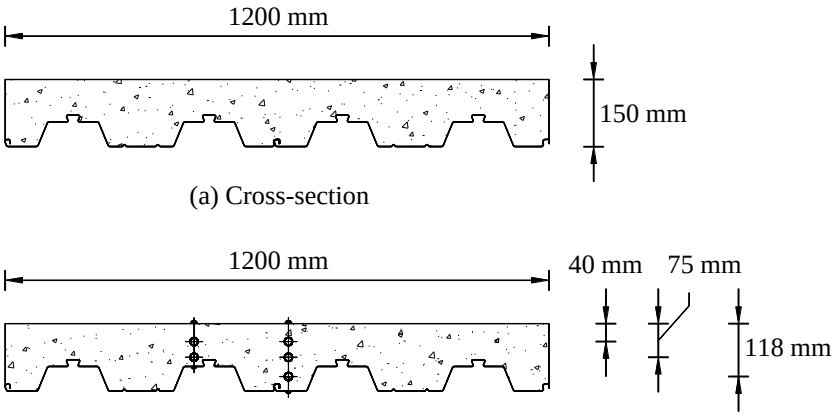

Figure 3. Cross-sections and embedded strain gages location in KF70 slabs

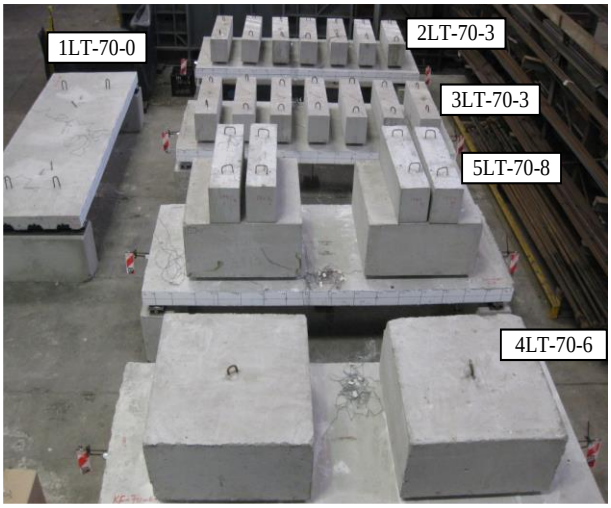

Figure 4. View of slabs with KF70 decking under sustained load

Loading Procedure

Each of the KF70 slabs was placed onto its supports at age 7 days and remained unloaded (except for its self-weight, see Table 1) until age 64 days. At age 64 days, with the exception of 1LT-70-0, each slab was subjected to superimposed sustained loads in the form of concrete blocks. Each concrete block was placed on 60 mm high timber blocks to ensure a largely uninterrupted air flow over the top surface of the slabs and allow the concrete to shrink freely on the top surface. The block layouts are illustrated in Fig. 5 (and are also shown in the photograph of Fig. 4). Slab 1LT-70-0 carried only self-weight for the full test duration of 240 days. Slabs 2LT-70-3 and 3LT-70-3 were identical, carrying a constant superimposed sustained load of 3.4 kPa from age 64 days to 247 days, i.e. a total sustained load of 6.4 kPa. Slab 4LT-70-6 carried a constant superimposed sustained load of 6.0 kPa from age 64 days to 247 days, i.e. a total sustained load of 9.0 kPa. Slab 5LT-70-8 carried a constant superimposed sustained load of 6.1 kPa from age 64 days to 197 days, i.e. a total sustained load of 9.1 kPa and from age 197 days to 247 days the superimposed sustained load was 7.9 kPa , i.e. a total sustained load of 10.9 kPa.

Each of the KF40 slabs was placed onto the supports at age 7 days and remained unloaded except for its self-weight, i.e. 3.2 kPa until age 28 days. At age 28 days (after 21 days drying), with the exception of 6LT-40-0, each slab was subjected to superimposed sustained loads with the block layouts similar to that used for the KF70 slabs and shown in Fig. 5. Slab 6LT-40-0 carried only self-weight for the full test duration of 244 days. Slabs 7LT-40-3 and 8LT-40-3 were identical, carrying a constant superimposed sustained load of 3.4 kPa from age 28 days to 251 days, i.e. a total sustained load of 6.6 kPa. Slabs 9LT-40-6 and 10LT-40-6 were also identical and carried a constant superimposed sustained load of 6.4 kPa from age 28 days to 251 days, i.e. a total sustained load of 9.6 kPa.

[Downloaded from sjfst.srpub.org on 2026-09-16]

[DOI: 10.47176/sjfst.4.2.1]

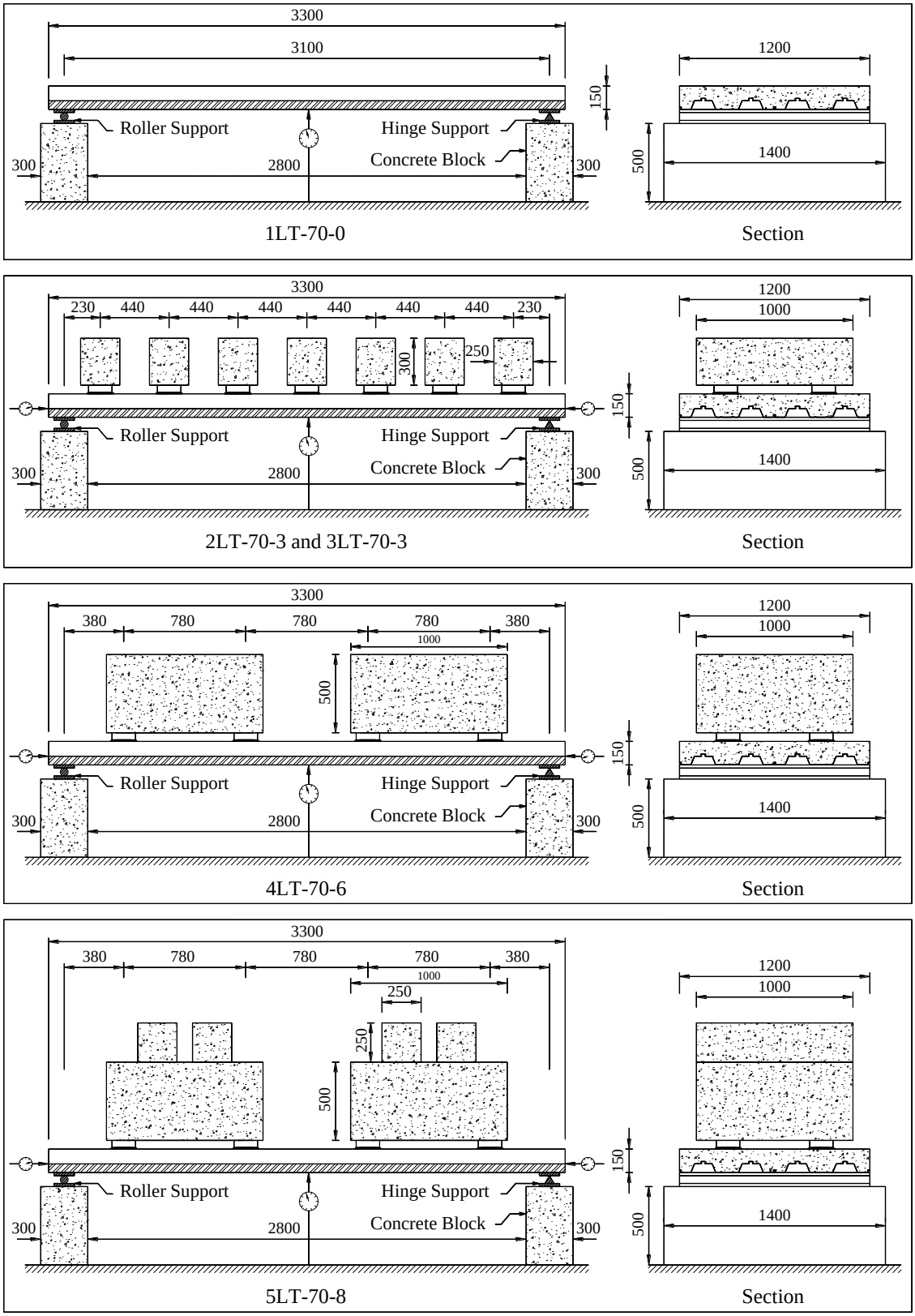

Figure 5. Sustained load configuration for KF70 slabs

[Downloaded from sjfst.srpub.org on 2026-09-16]

[DOI: 10.47176/sjfst.4.2.1]

Experimental Results

The measured compressive strength, modulus of elasticity and flexural tensile strength are presented in Table 2. The measured creep coefficient versus time curves for concrete cylinders cast with the KF70 slabs and first loaded at age 64 days and KF40 slabs first loaded at age 28 days is shown in Fig. 6. The creep coefficient at the end of test for the KF70 slabs was ϕ (247,64) = 1.62. For the KF40 slabs, the creep coefficient at the end of the test (age 251 days) for the concrete first loaded at age 28 days was ϕ (251,28) = 1.50.

The development of the drying shrinkage strain for the concrete is also shown in Fig. 6. The curves represent the average of the measured shrinkage on two standard shrinkage prisms, 75 mm × 75 mm × 275 mm, from the day after removing the wet hessian until the end of the test. The average measured shrinkage strain at the end of test for the KF70 slabs was ε_{sh} = 512 με. Similarly, for the KF40 slabs, the average measured shrinkage strain at the end of tests was ε_{sh} = 630 με.

The average of the measured values of yield stress and elastic modulus taken from three test samples of the KF70 decking were f_y = 544 MPa and E_{sd} = 212 GPa, respectively. Similarly, from three test samples of the KF40 decking, average values were f_y = 475 MPa and E_{sd} = 193 GPa, respectively.

Table 2
Concrete properties

Slab Type	f'_c (MPa)		E_c (MPa)		$f_{ct.f}$ (MPa)	
KF70	64 days	28.0	64 days	30725	64 days	3.50
	247 days	29.8	247 days	31650	247 days	4.54
KF40	28 days	35.5	28 days	28200	28 days	3.80
	251days	42.7	251 days	31600	251 days	5.05

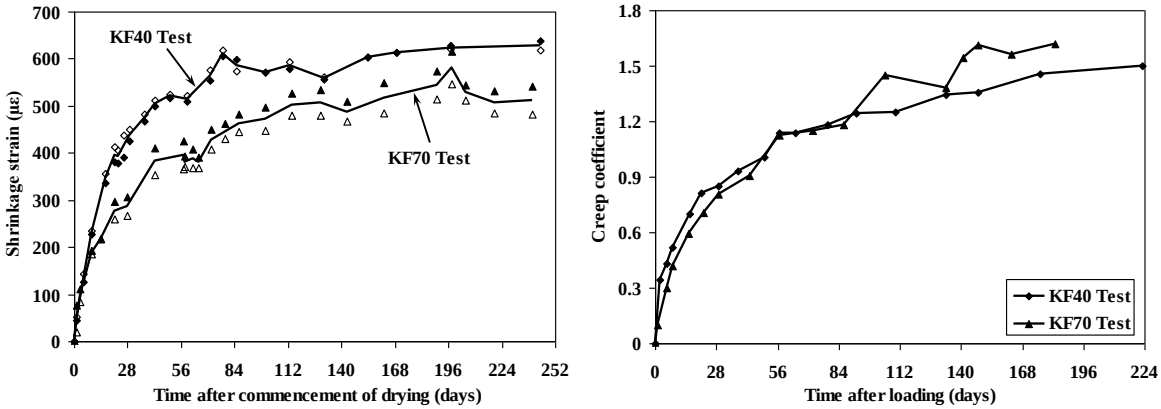

Figure 6. Creep coefficient and shrinkage strain versus time

Mid-span Deflection and End Slip

The variations of mid-span deflection with time for the KF70 and KF40 slabs are shown in Fig. 7. Key deflection values are summarized in Table 3. The measured deflection includes that caused by shrinkage, the creep induced deflection due to the sustained load (including self-weight), the short-term deflection caused by the superimposed loads (blocks) and the deflection caused by the loss of stiffness resulting from time-dependent cracking (if any). It does not include the initial deflection of the uncracked slab at age 7 days due to self-weight (which has been calculated to be about 0.5 mm for both the KF70 and KF40 slabs).

The measured end slips were very small with the maximum values of about 0.1 mm and 0.12mm at the supports in 3LT-70-3 & 4LT-70-6, respectively. The end slips were negligible in the other slabs.

[Downloaded from sjfst.srpub.org on 2026-09-16]

[DOI: 10.47176/sjfst.4.2.1]

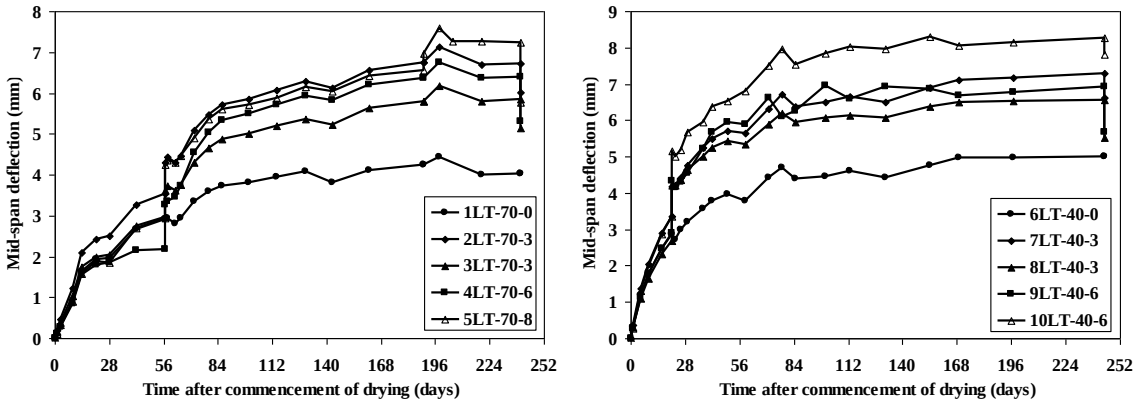

Figure 7. Mid-span deflection versus time

Discussion of Test Results

Shrinkage clearly has a dominant effect on the final deflection of these composite slabs. With a sustained load of 3.2 kPa (self-weight), the final deflection of 6LT-40-0 was 4.99 mm. When the sustained load was increased by a factor of about 3 to 9.6 kPa, the slabs suffered additional cracking and yet the final deflection only increased by a factor of about 1.4 to 6.94 mm (9LT-40-6) and by a factor of about 1.7 to 8.26 mm (10T-40-6). A similarly dominant effect of shrinkage over load was observed in the KF70 slabs.

Prior to the application of any load other than self-weight, the slabs deflected significantly, mainly due to the shrinkage-induced curvature. For the five KF70 slabs, after 57 days of drying (when ε_{sh} = 400 με), the deflection varied from 2.18 mm (for 4LT-70-6) to 3.54 mm (for 2LT-70-3). Although this was mainly due to early shrinkage, it included the creep deflection resulting from self-weight which was estimated at about 0.4 mm. At this stage all KF70 slabs were identical (in terms of materials, geometry and load history), yet the deflection varied significantly. This highlights the large degree of variability when considering the service load behavior of concrete slabs, with deflection being highly dependent on the non-linear and time-dependent behavior of the concrete. For the five KF40 slabs, after 21 days of drying (when ε_{sh} = 390 με), the deflection varied from 2.72 mm (for 8LT-40-3) to 3.33 mm (for 7LT-40-3).

The difference in the extent of time-dependent cracking between the KF70 slabs and the KF40 slabs was somewhat unexpected. With the centroid of the KF40 steel decking being only 14 mm above the bottom of the slab (and that of the KF70 decking being 27.7 mm above the bottom), the tensile force that developed with time on the concrete, due to the restraint provided by the KF40 decking to drying shrinkage, is significantly more eccentric to the centroid of the concrete than that provided by the KF70 decking. This will increase the concrete tensile stress in the bottom fibers of the concrete and may have contributed to the observed differences in crack patterns.

Table 3
Measured mid-span deflections

	Time-dependent deflection (mm)					
	57days of drying		190 days of drying		240 days of drying	
Slab	Before	After	Before	After	Before	After
1LT-70-0	2.92	2.92	4.24	4.24	4.04	4.04
2LT-70-3	3.54	4.29	6.74	6.74	6.72	6.01
3LT-70-3	2.97	3.63	5.80	5.80	5.84	5.16
4LT-70-6	2.18	3.38	6.37	6.37	6.40	5.31
5LT-70-8	2.94	4.23	6.56	6.96	7.23	5.78
	Time-dependent deflection (mm)					
	21 days of drying		28 days	56 days	244 days of drying	
Slab	Before	After	of drying	of drying	Before	After
6LT-40-0	2.83	2.83	3.15	3.87	4.99	4.99
7LT-40-3	3.33	4.14	4.72	5.68	7.30	6.62
8LT-40-3	2.72	4.12	4.70	5.38	6.57	5.53
9LT-40-6	2.95	4.35	4.60	5.90	6.94	5.68
10LT-40-6	3.30	5.10	5.52	6.72	8.26	7.81

[Downloaded from sjfst.srpub.org on 2026-09-16]

[DOI: 10.47176/sjfst.4.2.1]

Analytical Modeling

An analytical procedure for the time-dependent analysis of composite concrete cross-sections with uniform shrinkage through the thickness of the concrete slab and with full interaction was presented by Gilbert and Ranzi [9] using the age-adjusted effective modulus method [13-14]. Gilbert et al. [1] extended the method to calculate the effects of a non-uniform shrinkage gradient by layering the concrete cross-section, with the shrinkage strain specified in each concrete layer depending on its position within the cross-section and with the assumption of full shear interaction at service load levels. This method is adopted here.

To calculate the time-dependent deformation of a composite concrete cross-section, the shrinkage strain profile and the creep coefficient for the concrete slab are needed. In the following, a shrinkage strain profile is proposed for concrete slabs on profiled steel decking that is suitable for use in structural design and a modification to the provisions of Bažant-Baweja B3 prediction model [10] for estimating the shrinkage strain and creep coefficient for composite slabs is also proposed. The proposals have been developed empirically from experimental measurements of shrinkage induced strain distributions in composite slabs.

For a composite slab on profiled steel decking, if the average thickness of the concrete t_{ave} is defined as the area of the concrete part of the cross-section A_c divided by the width of the cross-section b, the following modifications to the term V/S is proposed to account for the effect of the steel decking on the drying profile through the concrete and hence on the magnitude of creep and shrinkage:

$$V/S = 25 + 0.25t_{ave} \text{ (in mm)} \quad (1)$$

For the decking profiles considered in this study, the ratio of trough height to slab thickness is defined as r_d (as described in Fig. 8) and was in the range 0.25 to 0.5. The modification factor K_m for creep coefficient and shrinkage strain is proposed as:

$$K_m = 1.5 - 0.55r_d \quad (2)$$

$$\varepsilon^{*}_{sh}(t,t_c) = K_m \varepsilon_{sh}(t,t_c) \quad (3)$$

$$\phi^{*}(t,t_0) = K_m \phi(t,t_0) \quad (4)$$

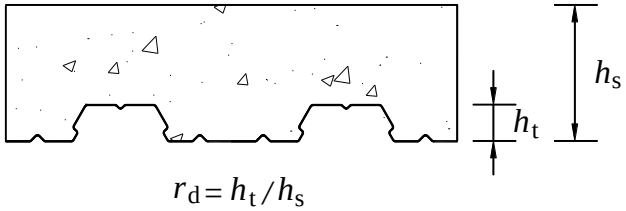

Figure 8. Definition of shape factor (r_d)

The measured shrinkage strain at any height y above the soffit of the composite slab with overall depth D, $\varepsilon_{sh}(y)$, may be approximated by Eq. 31:

$$\frac{\varepsilon_{sh}(y)}{\varepsilon^{*}_{sh}(t,t_c)} = \alpha + \beta\left(\frac{y}{D}\right)^4 \quad (5)$$

where $\varepsilon_{sh}(0) = \alpha \varepsilon^{*}_{sh}(t,t_c)$ is the shrinkage strain at the bottom of the slab (at y = 0) and $\varepsilon_{sh}(D) = (\alpha+\beta)\varepsilon^{*}_{sh}(t,t_c)$ is the shrinkage strain at the top surface of the slab (at $y = D$).

From the experimental results, α = 0.2 provides a reasonable estimate, but β appears to depend on the profile of the steel decking. Excellent agreement between the predicted long-term deflection and the measured values is obtained with the value of $\beta = 2.0 - 2.25r_d$ as shown in Fig. 9 and Fig. 10.

The analytical curves were obtained by double integration of the curvature diagram at each time instant, with the curvature determined at cross-sections at 155 mm centers along the span using the layered cross-section approach of Gilbert et al. [1]. Sample calculations for the determination of the short-term and time-dependent curvature at mid-span of slab 1LT-70-0 are provided in the Appendix, together with the determination of the shrinkage profile through the thickness of the slab.

For each slab, the same load history was considered in the analytical modeling as was applied to the real slab. Where two identical slabs with identical loading histories were tested, the analytical deflection-time curves are compared with the average of the two experimental curves. In those parts of the slabs where the numerical study showed that cracking had occurred, the effect of tension stiffening was considered using an approach similar to that outlined in Eurocode 2 [15]. The average curvature (κ_{ave}) used in deflection calculation is determined according to Eq. 32:

$$\kappa_{ave} = \zeta\kappa_{cr} + (1-\zeta)\kappa_{uncr} \quad (6)$$

where κ_{cr} is the time-dependent curvature on the cracked cross-section (ignoring tension in the concrete); κ_{uncr} is the time-dependent curvature on the

[Downloaded from sjfst.srpub.org on 2026-09-16]

[DOI: 10.47176/sjfst.4.2.1]

uncracked cross-section; and ζ is the distribution coefficient given by:

$$\zeta = 1 - \left(\frac{M_{cr,t}}{M_s} \right)^2 \quad (7)$$

where $M_{cr,t}$ is the cracking moment at the time under consideration and M_s is the in-service moment imposed on the cross-section.

The shrinkage induced deflection calculated using the proposed shrinkage profile for each decking type (Eq. 31), together with the instantaneous and time-dependent deflection caused by the applied load (elastic and creep deflection), are in good agreement with the measured response of the slabs.

A summary of the measured and calculated mid-span deflections is presented in Table 4, where comparisons between the measured and predicted deflections are made at 42 days after the commencement of drying and at the end of the test.

Table 4
Measured and calculated mid-span deflections

	Time-dependent deflection, mm (in.)					
	42 days of drying			240 days of drying		
Slab	Measured (test)	Calculated	Measured/ Calculated	Measured (test)	Calculated	Measured/ Calculated
1LT-70-0	2.67	2.86	0.93	4.04	5.05	0.80
2LT-70-3	3.27	2.86	1.14	6.72	6.36	1.06
3LT-70-3	2.74	2.86	0.96	5.84	6.36	0.92
4LT-70-6	2.16	2.86	0.76	6.40	7.38	0.87
5LT-70-8	2.69	2.86	0.94	7.23	8.74	0.83
	Time-dependent deflection, mm (in.)					
	42 days of drying			244 days of drying		
Slab	Measured (test)	Calculated	Measured/ Calculated	Measured (test)	Calculated	Measured/ Calculated
6LT-40-0	3.77	3.13	1.20	4.99	5.70	0.88
7LT-40-3	5.50	4.16	1.32	7.30	7.04	1.04
8LT-40-3	5.26	4.16	1.26	6.57	7.04	0.93
9LT-40-6	5.67	5.76	0.98	6.94	8.47	0.82
10LT-40-6	6.36	5.76	1.10	8.26	8.47	0.98

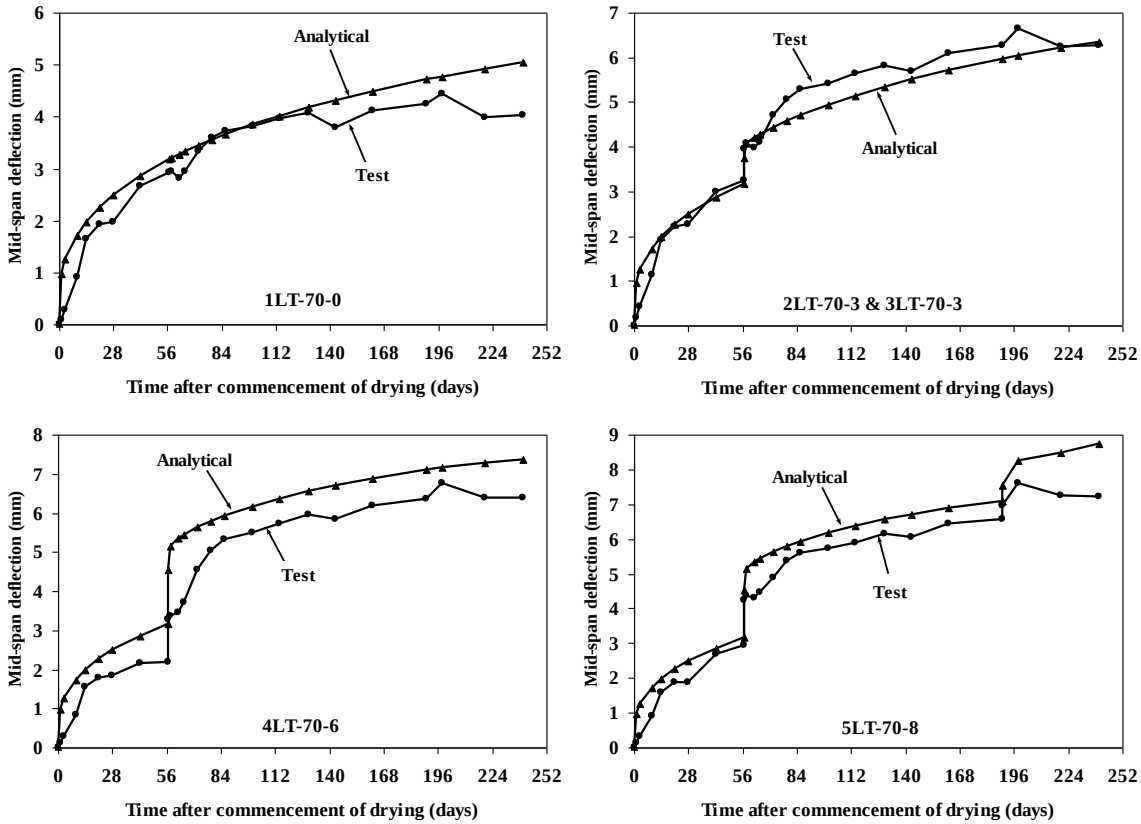

Figure 9. Mid-span deflection versus time (KF70 slabs)

[Downloaded from sjfst.srpub.org on 2026-09-16]

[DOI: 10.47176/sjfst.4.2.1]

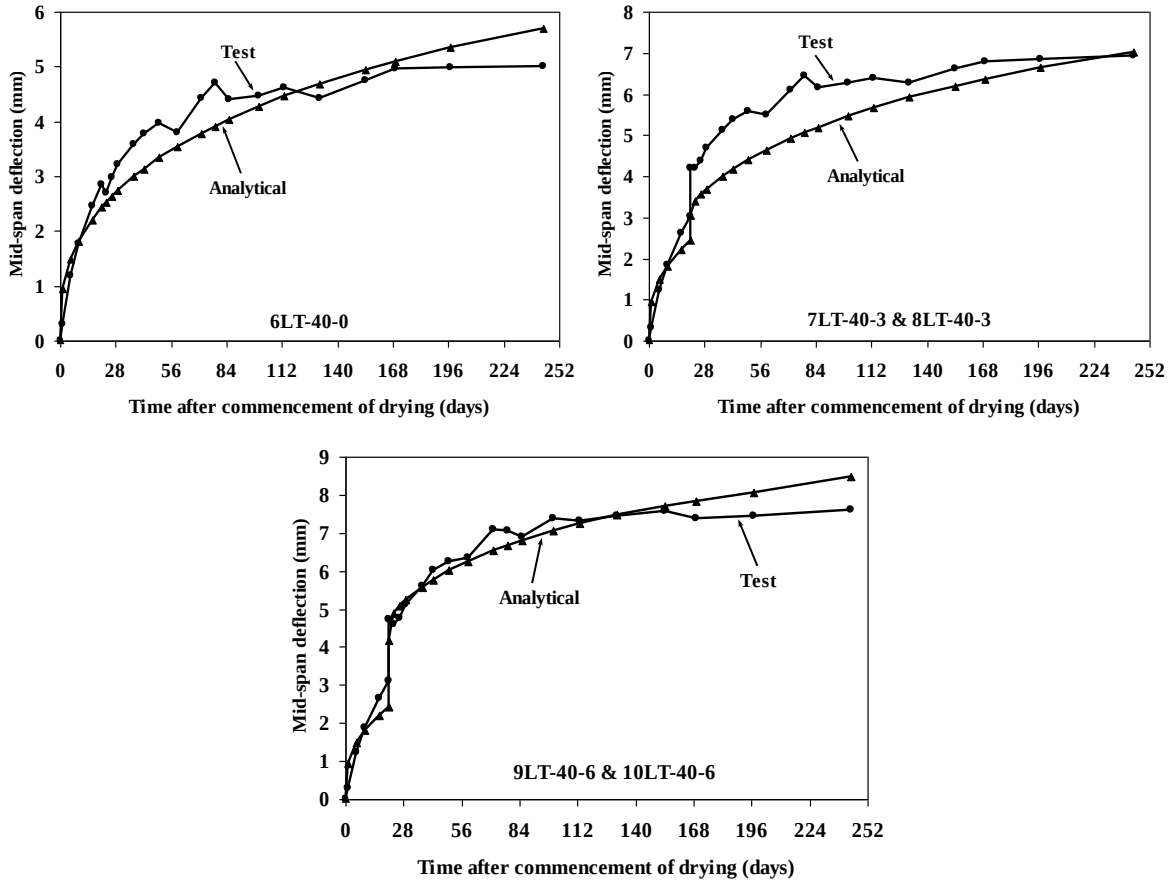

Figure 10. Mid-span deflection versus time (KF40 slabs)

Summary and Conclusions

The results of an experimental study of the long-term deflection of composite concrete slabs under sustained loads have been presented. The deformation caused by applied load, creep of the concrete and the effects of drying shrinkage have been reported and discussed for ten simply-supported slabs, with either KF70 or KF40 steel decking [10], subjected to different loading histories. The measured slab deflections have confirmed the dominant effect of drying shrinkage over load for normal levels of sustained loads.

Also proposed is a non-linear shrinkage profile through the thickness of a composite concrete slab, together with an analytical model for calculating the instantaneous and time-dependent curvature of the cross-section due to the effects of both load and non-linear shrinkage. The agreement between the calculated deflection and the measured deflection for each of the ten slabs is good.

Appendix - Sample Calculations

Sample calculations of the short-term and long-term curvature on the cross-section of slab 1LT-70-0 at mid-span are presented here using the approach presented by Gilbert et al. [1]. The slab was simply-supported over a span of 3100 mm and loaded with its self-weight of 3.60 kN/m at age 7 days. That uniform load remained constant for a further period of 240 days, with deformation increasing with time due to creep and shrinkage. The cross-section of the slab is divided into 10 layers, each 15 mm thick as shown in Fig. 11. Details of the geometric discretization are presented in Table 5. For this slab the elastic modulus of the concrete is assumed to be constant as E_c = 30.73 GPa and for the steel decking E_s = 212 GPa.

[Downloaded from sjfst.srpub.org on 2026-09-16]

[DOI: 10.47176/sjfst.4.2.1]

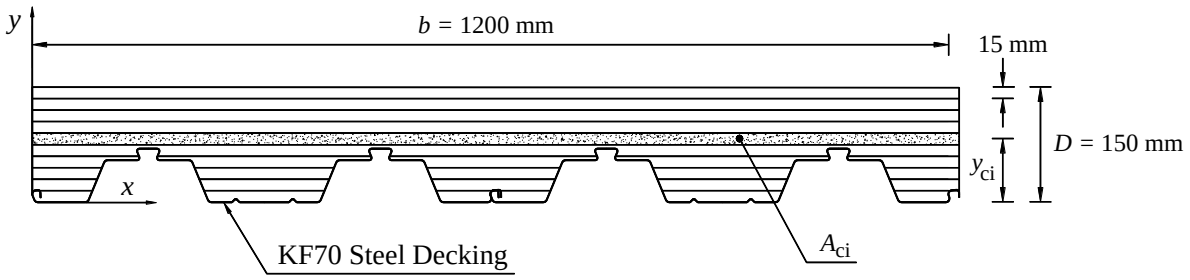

A_{sd} = 1320 mm^2

y_{sd} = 27.7 mm

Figure 11. Geometry and analysed cross-section of slab 1LT-70-0

For this lightly loaded slab, the maximum sustained bending moment at mid-span is M_{max} = 4.32 kNm. The average thickness of the concrete is $t_{ave} = A_c/b$ = 148.8×10^3/1200 = 124 mm. Take $t_c = t_0$ = 7 days, t = 247 days, f_c = 28 MPa, $f_{cm28} = f_c$ +8.3=36.3 MPa, E_{cm28} = 30.73 GPa, a_1 = 1.0, a_2 = 1.2, c = 400 kg/m^3, w = 200 kg/m^3, a = 1650 kg/m^3, RH = 67%, k_s = 1.0

Calculation of shrinkage strain in each concrete layer:

$$E_{cm607} = E_{cm28}\left(\frac{607}{4+0.85\times 607}\right)^{0.5} = 33.20 \text{ Gpa}$$

and with t_c = 7 days and

$V/S = 25 + 0.25t_{ave} = 56$ mm,

$\tau_{sh} = 0.085\times 7^{-0.08}\times 36.3^{-0.25}[2\times 1\times 56]^2 = 371.7$

$$E_{cm(t_c+\tau_{sh})} = E_{cm28}\left(\frac{378.7}{4+0.85\times 378.7}\right)^{0.5} = 33.1 \text{ Gpa}$$

$\varepsilon_{su} = 1\times 1.2\times[0.019\times 200^{2.1}\times 36.3^{-0.28}+270]\times 10^{-6} = 891\times 10^{-6}$

$S(t-t_c) = \tanh\sqrt{\frac{(247-7)}{371.7}} = 0.67$,

$k_h = 1-\left(\frac{67}{100}\right)^3 = 0.7$,

$\varepsilon_{shu} = 891\times 10^{-6}\times\frac{33.2}{33.1} = 894\times 10^{-6}$

$\varepsilon_{sh}(t,t_c) = 894\times 10^{-6}\times 0.7\times 0.67 = 419\times 10^{-6}$,

$K_m = 1.5 - 0.55r_d = 1.5 - 0.55\times\frac{70}{150} = 1.24$

$\varepsilon^*_{sh}(t,t_c) = K_m\varepsilon_{sh}(t,t_c) = 1.24\times 419\times 10^{-6} = 520\times 10^{-6}$

, $\beta = 2.0 - 2.25r_d = 2 - 2.25\times\frac{70}{150} = 0.95$

The shrinkage strain at the centroid of the i-th concrete layer on the cross-section is obtained from Eq. 5:

$$\varepsilon_{sh}(y_{ci}) = \varepsilon^*_{sh}(t,t_c)\times\left(\alpha+\beta\left(\frac{y_{ci}}{D}\right)^4\right) = -520\times\left(0.2+0.95\left(\frac{y_{ci}}{150}\right)^4\right)$$

and is listed in Table 5.

Table 5
Area, position and shrinkage strain of concrete layers

Layer (i)	$A_{c(i)}$ (mm^2)	y_{ci} (mm)	ε_{sh}
1	8768	7.5	-104.0×10^{-6}
2	9710	22.5	-104.3×10^{-6}
3	10446	37.5	-105.9×10^{-6}
4	12917	52.5	-111.4×10^{-6}
5	16922	67.5	-124.3×10^{-6}
6	18000	82.5	-149.2×10^{-6}
7	18000	97.5	-192.2×10^{-6}
8	18000	112.5	-260.3×10^{-6}
9	18000	127.5	-361.9×10^{-6}
10	18000	142.5	-506.4×10^{-6}
Σ	148763		

[Downloaded from sjfst.srpub.org on 2026-09-16]

[DOI: 10.47176/sjfst.4.2.1]

Calculation of Creep Coefficient:

$$q_2 = 185.4\times10^{-6}\times400^{0.5}\times36.3^{-0.9} = 146.3\times10^{-6}$$

$$Q_f(t_0) = \left[0.086\times7^{2/9} + 1.21\times7^{4/9}\right]^{-1} = 0.33,$$

$$Z(t,t_0) = 7^{-0.5}\times\ln\left[1+(247-7)^{0.1}\right] = 0.38,$$

$$r(t_0) = 1.7\times7^{0.12} + 8 = 10.15$$

$$q_3 = 0.29(200/400)^4 146.3\times10^{-6} = 2.7\times10^{-6},$$

$$q_4 = 20.3\times(1650/400)^{-0.7}\times10^{-6} = 7.5\times10^{-6}$$

$$Q(t,t_0) = 0.33\times\left[1+\left(\frac{0.33}{0.38}\right)^{10.15}\right]^{-1/10.15} = 0.32$$

$$C_0(t,t_0) = 146.3\times10^{-6}\times0.32 + 2.7\times10^{-6}\times\ln[1+(247-7)^{0.1}] + 7.5\times10^{-6}\times\ln\left(\frac{247}{7}\right) = 76.3\times10^{-6}$$

$$S(t_0-t_c) = 0,\ H(t_0) = 1,$$

$$H(t) = 1-(1-0.67)\times0.67 = 0.78$$

$$q_5 = 0.757\times36.3^{-1}\times894^{-0.6} = 353\times10^{-6}$$

$$C_d(t,t_0,t_c) = 353\times10^{-6}\times[e^{-8\times0.78} - e^0]^{0.5} = 14\times10^{-6}$$

And the creep coefficient at age 247 days due to loading first applied at t_0 = 7 days is:

$$\phi(t,t_0) = 30.73\times10^3\times\left(76.3\times10^{-6} + 14\times10^{-6}\right) = 2.77$$

$$\phi^*(t,t_0) = 1.24\times2.77 = 3.43$$

Short-term analysis at mid-span at t_0 = 7 days:

The strain at any point on the cross-section y above the slab soffit at time t_0 = 7 days, immediately after first loading can be expressed as $\varepsilon = \varepsilon_{r,0} - y\kappa_0$, where $\varepsilon_{r,0}$ is the strain at the slab soffit and κ_0 is the instantaneous curvature. Following the approach outline by Gilbert et al. [1], the strain at mid-span due to any combination of axial force N_0 and moment M_0 is:

$$\begin{bmatrix}\varepsilon_{r,0}\\ \kappa_0\end{bmatrix} = \frac{1}{R_{A,0}R_{I,0} - R_{B,0}^2}\begin{bmatrix}R_{I,0} & R_{B,0}\\ R_{B,0} & R_{A,0}\end{bmatrix}\times\begin{bmatrix}N_0\\ M_0\end{bmatrix} \quad (8)$$

where $R_{A,0}$, $R_{B,0}$ and $R_{I,0}$ are the rigidities of the transformed section related to area, first moment of area and second moment of area about the slab soffit and are calculated as:

$$R_{A,0} = \sum_{i=1}^{10} A_{ci}E_c + E_{sd}A_{sd} = 4851\times10^6 \text{ N}$$

$$R_{B,0} = \sum_{i=1}^{10} y_{ci}A_{ci}E_c + y_{sd}A_{sd}E_{sd} = 396\times10^9 \text{ Nmm}$$

$$R_{I,0} = \sum_{i=1}^{10} y_{ci}^2A_{ci}E_c + (y_{sd}^2A_{sd} + I_{sd})E_{sd} = 40.7\times10^{12} \text{ Nmm}^2$$

When N_0 = 0 and M_0 = 4.32 kNm, Eq. (10) gives:
$\varepsilon_{r,0}$ = 42.1×10^{-6} and κ_0 = 0.52×10^{-6} mm^{-1}.

The strain in the bottom concrete layer at y = 0 mm is $\varepsilon = \varepsilon_{r,0} - y\kappa_0$ = 42.1×10^{-6} and the corresponding concrete stress is $\sigma_c = \varepsilon E_c$ = 1.3 MPa. Since this is well below the tensile strength of concrete, this slab has not cracked at this time.

Long-term analysis at mid-span at t_k = 247 days:

Adopting the age-adjusted effective modulus method as outlined by Gilbert et al. [1], with an aging coefficient of $\chi(t_k,t_0) = 0.65$, the age-adjusted modulus for concrete after 240 days under load is:

$$\bar{E}_{e,k} = \frac{E_c}{1+\chi(t_k,t_0)\phi(t_k,t_0)} = \frac{30725}{1+0.65\times3.43} = 9514 \text{ MPa}$$

The strain at any point on the cross-section y above the slab soffit at time t_k = 247 days can be expressed as $\varepsilon = \varepsilon_{r,k} - y\kappa_k$, where $\varepsilon_{r,k}$ is the strain at the slab soffit and κ_k is the curvature at time t_k. Following the approach outline by Gilbert et al. [1], the strain at mid-span due to any combination of sustained axial force N_k and moment M_k is:

$$\begin{bmatrix}\varepsilon_{r,k}\\ \kappa_k\end{bmatrix} = \frac{1}{R_{A,k}R_{I,k} - R_{B,k}^2}\begin{bmatrix}R_{I,k} & R_{B,k}\\ R_{B,k} & R_{A,k}\end{bmatrix}\times(\mathbf{r}_k - \mathbf{f}_{cr,k} + \mathbf{f}_{sh,k}) \quad (9)$$

where $R_{A,k}$, $R_{B,k}$ and $R_{I,k}$ are the rigidities of the age-adjusted transformed section related to area, first moment of area and second moment of area about the slab soffit and are calculated as:

$$R_{A,k} = \sum_{i=1}^{10} A_{ci}\bar{E}_{e,k} + E_{sd}A_{sd} = 1695\times10^6 \text{ N}$$

$$R_{B,k} = \sum_{i=1}^{10} y_{ci}A_{ci}\bar{E}_{e,k} + y_{sd}A_{sd}E_{sd} = 128\times10^9 \text{ Nmm}$$

$$R_{I,k} = \sum_{i=1}^{10} y_{ci}^2A_{ci}\bar{E}_{e,k} + (y_{sd}^2A_{sd} + I_{sd})E_{sd} = 12.8\times10^{12} \text{ Nmm}^2$$

The vectors $\mathbf{r}_k$, $\mathbf{f}_{cr,k}$ and $\mathbf{f}_{sh,k}$ are vectors of axial force and moment: with $\mathbf{r}_k$ consisting of N_k and M_k; $\mathbf{f}_{cr,k}$ contains the fictitious actions resulting from the change in strain caused by creep due to the initial concrete stress at age t_0 and assuming full restraint; and $\mathbf{f}_{sh,k}$ contains the actions if the shrinkage strain was completely restrained over the time period.

$$\mathbf{f}_{cr,k} = \sum_{i=1}^{m_c}\bar{F}_{e(i),0}\begin{bmatrix}N_{c(i),0}\\ M_{c(i),0}\end{bmatrix} = \sum_{i=1}^{m_c}\bar{F}_{e(i),0}\,E_{c(i),0}\begin{bmatrix}A_{c(i)}\varepsilon_{r,0} - B_{c(i)}\kappa_0\\ -B_{c(i)}\varepsilon_{r,0} + I_{c(i)}\kappa_0\end{bmatrix} \quad (10)$$

$$\mathbf{f}_{sh,k} = \sum_{i=1}^{m_c}\begin{bmatrix}A_{c(i)}\\ -B_{c(i)}\end{bmatrix}\bar{E}_{e(i),k}\varepsilon_{sh(i),k} \quad (11)$$

where the terms $A_{c(i)}$, $B_{c(i)}$ and $I_{c(i)}$ are the area, the first and second moments of area of the i-th concrete layer about the x-axis, respectively.In this case:

[Downloaded from sjfst.srpub.org on 2026-09-16]

[DOI: 10.47176/sjfst.4.2.1]

$$\mathbf{r}_k = \begin{bmatrix} 0 \\ 4.32\times10^6 \ \text{Nmm} \end{bmatrix};$$

$$\mathbf{f}_{cr,k} = \begin{bmatrix} 3412 \ \text{N} \\ -1.72\times10^6 \ \text{Nmm} \end{bmatrix};\text{and}$$

$$\mathbf{f}_{sh,k} = \begin{bmatrix} -314\times10^3 \ \text{N} \\ 33.3\times10^6 \ \text{Nmm} \end{bmatrix}$$

and from Eq.9: $\varepsilon_{r,k}$ =183×10^{-6} and κ_k = 4.90×10^{-6} mm^{-1}.

Similar calculations may be formed at other cross-sections along the member and the curvature diagrams at times t_0 and t_k may be integrated to determine the slab deflection at each time, namely Δ_0 and Δ_k.

The curvatures so determined at ten points along the span are given in Table 6, where x_i is the distance of the section from the left end support of the slab.

Table 6
Calculated short-term and long-term curvatures

Section (i)	x_i (mm)	$\kappa_0 \times 10^{-6}$ (mm^{-1})	$\kappa_k \times 10^{-6}$ (mm^{-1})
0	0	0.00	3.10
1	155	0.10	3.44
2	310	0.18	3.75
3	465	0.26	4.02
4	620	0.33	4.25
5	775	0.38	4.45
6	930	0.43	4.61
7	1085	0.47	4.74
8	1240	0.49	4.83
9	1395	0.51	4.89
10	1550	0.52	4.90

Integration of the curvatures at each time instant gives the mid-span deflection:

Δ_0 = 0.51 mm and Δ_k = 5.52 mm

The time-dependent part of the mid-span deflection is therefore $\Delta_k^* = 5.52 - 0.51 = 5.01$ mm.

References

1. Gilbert RI, Bradford MA, Gholamhoseini A, Chang ZT. Effects of shrinkage on the long-term stresses and deformations of composite concrete slabs. *Eng Struct.* 2012; 40(July): 9-19.
2. Ranzi G, Ambrogi L, Al-Deen S, Uy B. Long-term experiments of post-tensioned composite slabs. *Proceedings of the 10th International Conference on Advances in Steel Concrete Composite and Hybrid Structures*, 2012; July: Singapore.
3. Al-deen S, Ranzi G. Effects of non-uniform shrinkage on the long-term behaviour of composite steel-concrete slabs. *Int J Steel Struct.* 2015; 15(2): 415-432.
4. Al-Deen S, Ranzi G, Vrcelj Z. Full-scale long-term and ultimate experiments of simply-supported composite beams with steel deck. *J Construct Steel Res.* 2011; 67(10): 1658-1676.
5. Ranzi G, Leoni G, Zandonini R. State of the art on the time-dependent behaviour of composite steel-concrete structures. *J Construct Steel Res.* 2013; 80(January): 252-263.
6. Carrier RE, Pu DC, Cady PD. Moisture distribution in concrete bridge decks and pavements. *Durability of Concrete, SP-47, American Concrete Institute*, Farmington Hills, Michigan, 1975; 169-192.
7. Bradford MA. Generic modelling of composite steel-concrete slabs subjected to shrinkage, creep and thermal strains including partial interaction. *Eng Struct.* 2010; 32(5): 1459-1465.
8. Gilbert RI. Deflection calculation for reinforced concrete structures - why we sometimes get it wrong. *ACI Struct J.* 1999; 96(6): 1027-1032.
9. Gilbert RI, Ranzi G. Time-dependent behavior of concrete structures. *Spon Press*, London. 2011; 426.
10. ACI Committee 209. Guide for modeling and calculating shrinkage and creep in hardened concrete (ACI 209.2R-08). *American Concrete Institute*, Farmington Hills, Michigan. 2008.
11. Standards Australia. Australian standard for concrete structures. *AS 3600-2009*, Sydney, Australia. 2009.
12. Fielders Australia PL. Specifying Fielders - KingFlor; Composite Steel Formwork System Design Manual. 2008.
13. Dilger W, Neville AM. Method of creep analysis of structural members. *ACI SP 27-17*, 1971; 349-379.
14. Bazant ZP. Prediction of creep effects using age-adjusted effective modulus method. *ACI Struct J.* 1972; 69(4): 212-217.
15. BS EN 1992-1-1. Eurocode 2: Design of Concrete Structures - Part 1-1: General Rules and Rules for Buildings, *British Standards Institution*, European Committee for Standardization, Brussels. 2004.

[Downloaded from sjfst.srpub.org on 2026-09-16]

[DOI: 10.47176/sjfst.4.2.1]

SJFST

Copyright: © 2022 The Author(s); This is an open-access article distributed under the terms of the Creative Commons Attribution License (http://creativecommons.org/licenses/by/4.0), which permits unrestricted use, distribution, and reproduction in any medium, provided the original work is properly cited.

Citation: Gholamhoseini A. A Creep and Shrinkage Prediction Model for Serviceability Analysis of Composite Concrete Slabs with Steel Decking. SJFST, 2022; 4(2): 1-14.

https://doi.org/10.47176/sjfst.4.2.1

[Downloaded from sjfst.srpub.org on 2026-09-16]

[DOI: 10.47176/sjfst.4.2.1]